Journal of ELECTRONIC MATERIALS, Vol. 38, No. 7, 2009
DOI: 10.1007/s11664-008-0630-1

Microstructure and Thermoelectric Properties of *n*- and *p*-Type Doped Mg_2Sn Compounds Prepared by the Modified Bridgman Method

H.Y. CHEN[1,2] and N. SAVVIDES[1]

1.—CSIRO Materials Science and Engineering, Sydney 2070, Australia. 2.—e-mail: haiyan.chen@csiro.au

Mg_2Sn compounds were prepared by the modified vertical Bridgman method, and were doped with Bi and Ag to obtain *n*- and *p*-type materials, respectively. Excess Mg was also added to some of the ingots to compensate for the loss of Mg during the preparation process. The Mg_2Sn samples were characterized by x-ray diffraction (XRD) and scanning electron microscopy (SEM), and their power factors were calculated from the Seebeck coefficient and electrical conductivity, measured from 80 K to 700 K. The sample prepared with 4% excess Mg, which contains a small amount of Mg_2Sn + Mg eutectic phase, had the highest power factor of 12×10^{-3} W m^{-1} K^{-2} at 115 K, while the sample doped with 2% Ag, in which a small amount of eutectics also exists, has a power factor of 4×10^{-3} W m^{-1} K^{-2} at 420 K.

Key words: Thermoelectric, Mg_2Sn, Bridgman method, microstructure, eutectic phase

INTRODUCTION

The Mg_2X (X = Si, Ge, Sn) semiconductor compounds and their solid solutions have received extensive attention as potential high-performance thermoelectric materials since the 1950s, and numerous investigations have been carried out regarding the electrical, optical, and thermal properties of Mg_2X.[1–6] The performance of a thermoelectric material is determined by the figure of merit $ZT = \alpha^2\sigma/\kappa$, where α is the Seebeck coefficient, σ is the electrical conductivity, and κ is the thermal conductivity. Vining[7] pointed out that ZT_{max} is proportional to the parameter $A = (T/300)(m^*/m_e)^{3/2}\ \mu/\kappa_L$, where m^* is the carrier effective mass, μ is the mobility in cm^2/V s, and κ_L is the lattice thermal conductivity in mW/cm K. In Mg_2X compounds A = 3.7 to 14, which is much larger than that of SiGe (A = 1.2 to 2.6) or β-$FeSi_2$ (A = 0.05 to 0.8), and thus Mg_2X should achieve higher ZT than SiGe. Zaitsev et al.[8] have reported ZT_{max} = 1.1 for bulk $MgSi_{0.4}Sn_{0.6}$ solid solution. Another advantage of Mg_2X is that their cost is low and they are environmentally friendly. However, research on Mg_2X is not as intense as on $CoSb_3$, PbTe, and SiGe alloys, due to the preparation and handling difficulties caused by the high vapor pressure and chemical reactivity of Mg.

Methods of direct co-melting,[9–11] mechanical alloying,[12–14] solid-state reaction,[15–17] and spark plasma sintering[18–20] have been used to prepare Mg_2X (X = Si, Ge, Sn) compounds and their solid solutions. Among these reported results, the method of direct co-melting followed by lengthy annealing used by Zaitsev et al.[8] showed the highest ZT values achieved to date. Herein we report the melt growth of Mg_2Sn crystalline ingots prepared by a modified Bridgman method. The microstructure and thermoelectric properties of pure and Ag-doped (*p*-type) or Bi-doped (*n*-type) Mg_2Sn are investigated and analyzed.

EXPERIMENT

High-purity Mg (4N), Sn (6N), Ag (3N), and Bi (6N) were mixed with the desired atom ratios as starting

(Received July 17, 2008; accepted December 12, 2008; published online January 6, 2009)

Table I. Atomic Ratios of Raw Materials

Sample	Atomic Ratio	
	Mg/Sn	Dopant
1	2.00:1	Undoped
2	2.04:1	Excess Mg
3	2.02:1	Bi 1%
4	2.02:1	Bi 2%
5	2.02:1	Ag 1%
6	2.02:1	Ag 2%

mixtures, as shown in Table I. Sample 1 was nominally stoichiometric, while excess Mg was added to the other samples to compensate for the evaporation of Mg during the melting and annealing processes. The mixtures were loaded into high-purity graphite crucibles with screw cover, and the charged crucibles were sealed in quartz ampoules under a gas mixture of Ar and H_2 at 0.8 MPa. The sealed quartz ampoules were suspended in a vertical tube furnace, which has a sharp temperature gradient at the bottom. The furnace was heated until the temperature of the quartz ampoule reached 1,093 K. After 30 min, the quartz ampoule was moved up and then down along the furnace at a fixed velocity for two cycles. The temperature gradient was about 1.8 K/mm at the liquid–solid interface. Thereafter the quartz ampoule was cooled to 573 K at a rate of 1 K/min, and then the ingot was annealed *in situ* at 573 K for 5 h.

The grown ingots were sliced using a diamond saw into several pieces with the desired dimensions. The crystalline structure of the samples was investigated using a Philips X'Pert PRO x-ray diffractometer and Cu Kα radiation. The microstructure was characterized using a JEOL JSM-5400 scanning electron microscope (SEM) fitted with an energy-dispersive x-ray (EDX) spectrometer. The electrical conductivity σ was measured by the four-point probe technique. The Seebeck coefficient α was measured in the temperature range of 80 K to 700 K using chromel–constantan thermocouples and copper voltage probes; the temperature difference at each measuring point was about 10 K to 15 K. During measurements the sample's temperature was raised at a rate of 1 K/min, and then furnace-cooled. The measurements were reproducible for both rising and falling temperatures.

RESULTS

The ingots were polycrystalline and easily cleaved. Excess Mg was observed in the top part of the ingots and a thin layer of Sn was evident at the very bottom of some ingots. Samples investigated in this work were cut from the middle parts of each ingot, avoiding where possible any sections that had free Mg or Sn or large voids. Nevertheless, most samples contained a number of very fine microcracks which are expected to lead to increased resistivity.

A comparison between the θ and 2θ x-ray diffraction spectra of the cleaved pellet and that of the crushed powder of sample 1 is shown in Fig. 1a. It is seen that the cleaved pellet of sample 1 has only (111), (222), and (511) diffraction peaks indicating some preferential orientation during growth while the powder sample shows all the expected diffraction peaks of cubic Mg_2Sn. Small amounts of free Sn were also detected in the crushed powders. It is known that some Mg is lost during melting due to its high vapor pressure. A very thin layer consisting of MgO + Si phases was found on the inner wall of the quartz ampoule indicating that Mg vapor permeates the graphite wall to react with the quartz. Figure 1b shows the x-ray patterns of the doped Mg_2Sn ingots. It is seen that all the samples are single-phase Mg_2Sn except for the small amount of free Mg in samples 2 and 6.

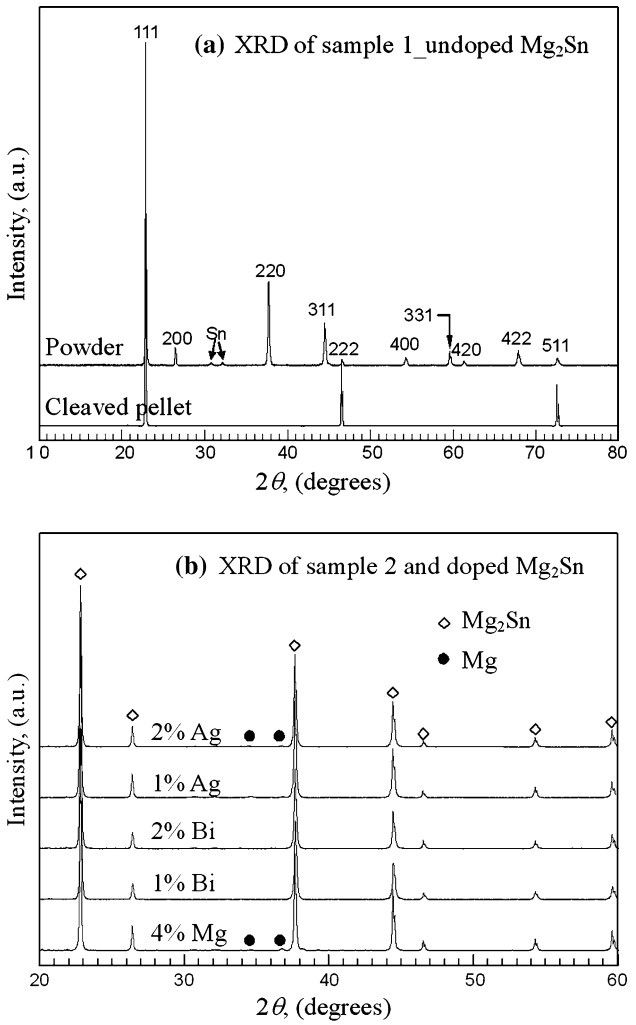

Fig. 1. X-ray spectra of (a) cleaved pellet and crushed powder of undoped Mg_2Sn, and (b) crushed powder of sample 2 and the doped Mg_2Sn ingots.

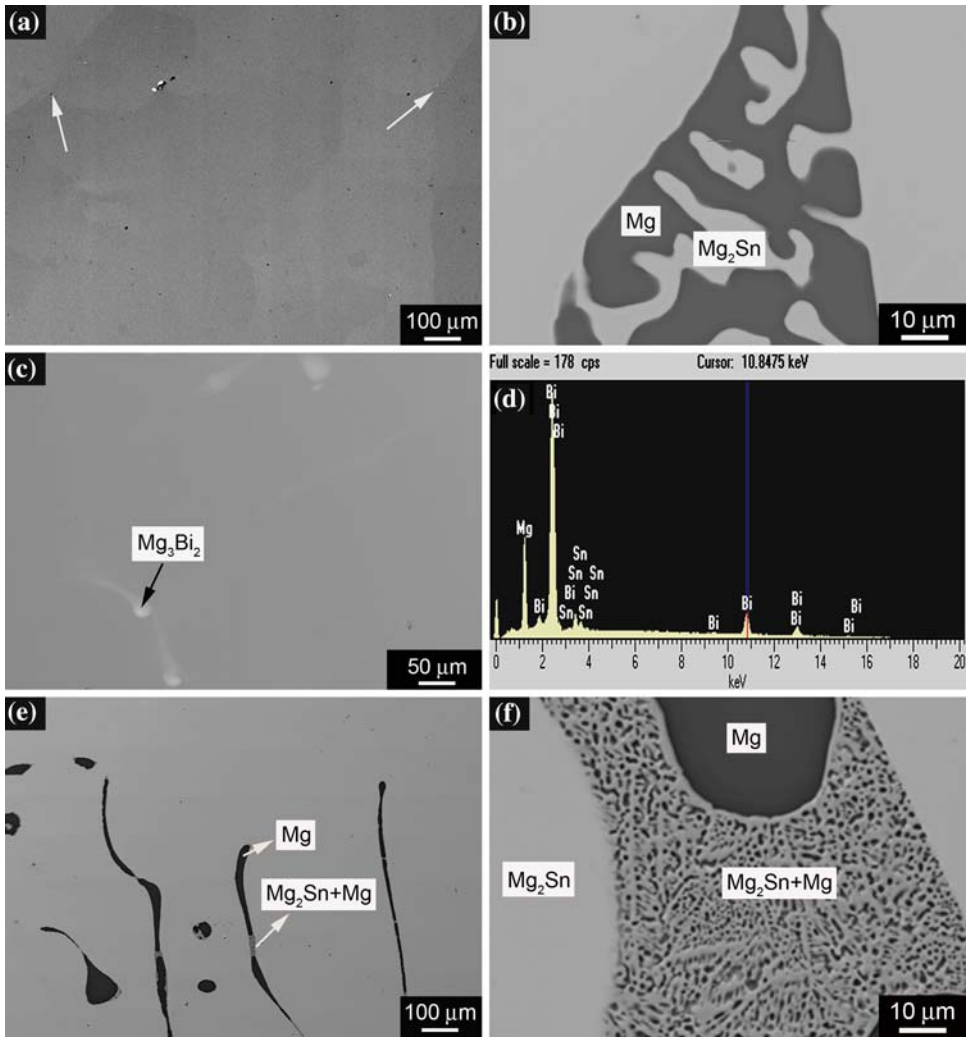

Fig. 2. SEM/EDX of Mg_2Sn ingots: (a) sample 1, (b) sample 2, (c) sample 4, (d) EDX of the bright phase of sample 4, (e) sample 5, and (f) sample 6.

Figure 2 shows SEM micrographs of the prepared samples; EDX was used to semiquantitatively analyze the chemical composition. Grain boundaries can be observed in Fig. 2a, confirming that sample 1 is polycrystalline. The bright particle in Fig. 2a is Sn precipitate. Mg_2Sn + Mg eutectic structures were observed in sample 2, as shown in Fig. 2b. The dark area in this structure was confirmed by EDX to be free Mg while the bright area and the whole of the matrix was single-phase Mg_2Sn. Samples 3 and 4 (Fig. 2c) have very similar microstructures, and from EDX analysis (Fig. 2d) the dispersed brighter phase is Mg_3Bi_2, which is reported to be a *p*-type thermoelectric compound.[21] Since no apparent diffraction peaks were detected by XRD, the amount of Mg_3Bi_2 should be very small. There exist also small amounts of free Mg and Mg_2Sn + Mg eutectic phase in samples 5 and 6, as shown in Fig. 2e and f.

Figure 3 shows the temperature dependence of the Seebeck coefficient α from 80 K to 700 K of all samples. At the lower temperatures the undoped sample 1 shows a transition from *p*- to *n*-type conduction, and is similar to observations by Zaitsev and Nikitin.[22] Higher temperatures lead to thermal

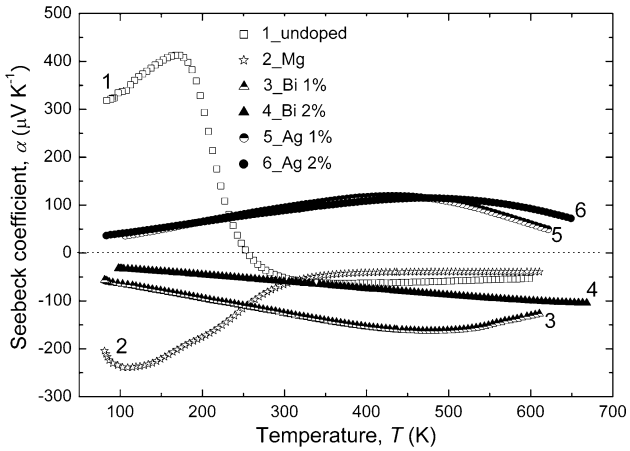

Fig. 3. Temperature dependence of Seebeck coefficients of Mg_2Sn ingots.

excitation of intrinsic charge carriers, and thus the Seebeck coefficient is characterized by weak temperature dependence. Sample 2 is also undoped except that it was prepared with excess Mg and shows n-type behavior in the whole temperature range of measurement with a similar α–T curve as that of pure Mg_2Sn reported by Winkler.[23] The peak in the value of α for both sample 1 and sample 2 at the lower temperatures is characteristic of lightly doped semiconductors where the rising thermal conductivity causes a phonon drag contribution to the Seebeck coefficient. The data for sample 1, containing excess Sn, and sample 2, containing excess Mg, are contrary to that given by Lichter,[24] who stated that Mg_2Sn crystals appear to dissolve the excess constituents, producing n-type crystals with excess Sn and p-type crystals with excess Mg. The doped ingot samples 3 and 4 (Bi doped) show n-type behavior in the whole temperature range of measurement, while the Ag-doped samples 5 and 6 are p-type. With the exception of sample 4, the absolute value of α first increases with increasing temperatures, reaches a broad peak at about 450 K, and then decreases at higher temperatures. Sample 4 appears to have a peak in α at temperature $T > 600$ K.

The electrical conductivity σ of the undoped sample 1 is plotted as a function of the reciprocal temperature in Fig. 4a. Our data is in very good agreement with that of single-crystal Mg_2Sn reported by Lichter[24] and Martin.[25] Figure 4b shows σ versus T for all the samples. The doped samples 3–6 show much higher σ values than the undoped sample 1, and their dependence on temperature is generally similar. Sample 2 with excess Mg shows similar behavior to the doped samples. The apparently high conductivity is due to the dispersed eutectic phase (Mg_2Sn + Mg) which forms from the free magnesium. In the doped samples the decrease of σ with rising temperature signifies the increasing role of phonon–electron and electron–electron scattering. It is noted, however, that the samples studied were not perfect specimens but rather contained both microcracks and voids, which decrease the measured conductivity. In addition, secondary phases such as free Mg or Sn and the eutectic structures would have a significant influence on the electrical conductivity. Thus, it is necessary to extend this study to include defect-free polycrystalline or single-crystal ingots of the Mg_2Sn compound.

The thermoelectric power factor, $P = \alpha^2\sigma$, calculated from the measured values of α and σ, is shown in Fig. 5. At temperatures suitable for practical applications (e.g., power generation) the doped samples 3–6 have useful power factors, with sample 6 reaching a peak value of about 4×10^{-3} W m^{-1} K^{-2} at 420 K. Despite its high α value at low temperatures, the undoped sample 1 has the lowest power factor. Sample 2, prepared with excess Mg, has a peak value of 12×10^{-3} W m^{-1} K^{-2} at 115 K due to the high Seebeck coefficient at low temperature caused by phonon drag, and high electrical conductivity due to the contribution of the eutectic phase. Using thermal conductivity values from the literature,[25] the highest figure of merit is obtained for sample 6, with $ZT_{max} \approx 0.45$ at 550 K.

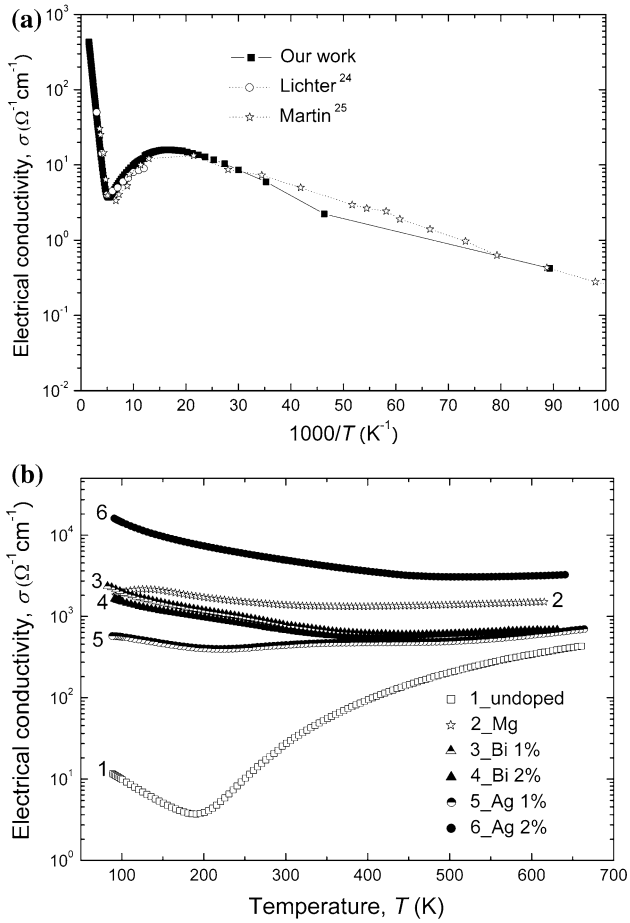

Fig. 4. Temperature dependence of electrical conductivity σ of Mg_2Sn ingots: (a) sample 1, (b) samples 1–6.

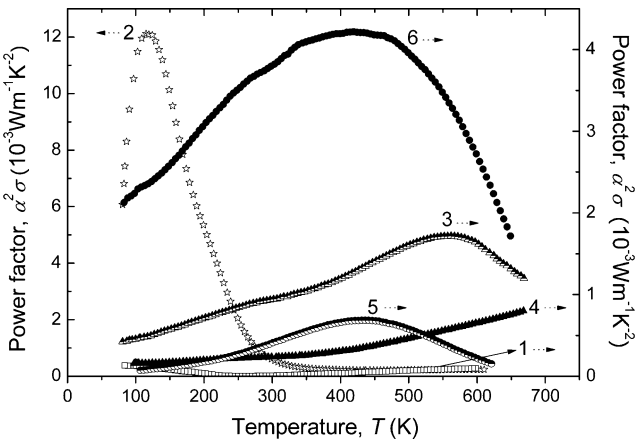

Fig. 5. Temperature dependence of power factor of Mg_2Sn ingots.

CONCLUSION

Ingots of the semiconducting compound Mg_2Sn were prepared from the melt by a modified Bridgman method. Bi-doped (n-type) and Ag-doped (p-type) materials were compared with undoped nominally stoichiometric material and with material with excess Mg. X-ray diffraction and EDX typically show ingots consisting of a uniform Mg_2Sn phase with minor quantities of the Mg_2Sn + Mg eutectic phase and small precipitates of Mg or Sn. Although the ingots contained many fine microcracks, measurements of the electrical conductivity and Seebeck coefficient in the temperature range 80 K to 700 K provide useful information on the thermoelectric properties of these materials. In particular, both the n-type and p-type ingots have broad Seebeck coefficient peaks with absolute values of 120 μV K^{-1} to 160 μV K^{-1} at T = 300 K to 600 K. Despite the presence of microcracks, these samples had useful power factors with the best value of about 4×10^{-3} W m^{-1} K^{-2} at around 400 K to 500 K.

REFERENCES

1. G. Busch and U. Winkler, *Helv. Phys. Acta* 26, 578 (1953).
2. R.G. Morris, R.D. Redin, and G.C. Danielson, *Phys. Rev.* 109, 1909 (1958). doi:10.1103/PhysRev.109.1909.
3. R.D. Redin, R.G. Morris, and G.C. Danielson, *Phys. Rev.* 109, 1916 (1958). doi:10.1103/PhysRev.109.1916.
4. R.J. Labotz and D.R. Mason, *J. Electrochem. Soc.* 110, 121 (1963). doi:10.1149/1.2425688.
5. J.J. Hauser, *Phys. Rev. B* 11, 3860 (1975). doi:10.1103/PhysRevB.11.3860.
6. Y. Noda, H. Kon, Y. Furukawa, I.A. Nishida, and K. Masumoto, *Mater. Trans. JIM* 33, 851 (1992).
7. C.B. Vining, *CRC Handbook of Thermoelectrics*, ed. D.M. Rowe (Boca Raton, USA: CRC Press, 1995), p. 277.
8. V.K. Zaitsev, M.I. Fedorov, E.A. Gurieva, I.S. Eremin, P.P. Konstantinov, A.Y. Samunin, and M.V. Vedernikov, *Phys. Rev. B.* 74, 045207.1 (2006).
9. E.N. Nikitin, V.G. Bazanov, and V.I. Tarasov, *Sov. Phys. Sol. St.* 3, 2648 (1962).
10. Y. Noda, H. Kon, Y. Furukawa, N. Otsuka, I.A. Nishida, and K. Masumoto, *Mater. Trans. JIM* 33, 845 (1992).
11. V.K. Zaitsev, M.I. Fedorov, I.S. Eremin, and E.A. Gurieva, *Thermoelectrics Handbook*, ed. D.M. Rowe (Boca Raton, USA: CRC Press, 2005), Ch. 29.
12. M. Riffel and J. Schilz, *Scr. Mater.* 32, 1951 (1995). doi:10.1016/0956-716X(95)00044-V.
13. J. Schilz, M. Riffel, K. Pixius, and H.J. Meyer, *Powder Technol.* 105, 149 (1999). doi:10.1016/S0032-5910(99)00130-8.
14. L. Lu, M.O. Lai, and M.L. Hoe, *Nano. Mater.* 10, 551 (1998). doi:10.1016/S0965-9773(98)00102-0.
15. R.B. Song, Y.Z. Liu, and T. Aizawa, *J. Mater. Sci. Technol.* 21, 618 (2005).
16. T. Aizawa and R. Song, *Mater. Sci. Forum* 536, 221 (2007).
17. T. Aizawa, R. Song, and A. Yamamoto, *Mater. Trans. JIM* 46, 1490 (2005). doi:10.2320/matertrans.46.1490.
18. T. Kajikawa, *Proceedings of the 16th International Conference on Thermoelectrics* (Piscataway, USA, 1997), p. 28.
19. T. Kajikawa, K. Shida, K. Shiraishi, and T. Ito, *Proceedings of the 17th International Conference on Thermoelectrics* (Nagoya, Japan, 1998), p. 362.
20. J. Tani and H. Kido, *Physica B* 364, 218 (2005). doi:10.1016/j.physb.2005.04.017.
21. T. Kajikawa, N. Kimura, and T. Yokoyama, *Proceedings of the 22nd International Conference on Thermoelectrics* (La Grande Motte, France, 2003), p. 305.
22. V.K. Zaitsev and E.N. Nikitin, *Sov. Phys. Solid State* 12, 289 (1970).
23. U. Winkler, *Helv. Phys. Acta* 28, 633 (1955).
24. B.D. Lichter, *J. Electrochem. Soc.* 109, 819 (1962). doi:10.1149/1.2425561.
25. J.J. Martin and G.C. Danielson, *Phys. Rev.* 166, 879 (1968). doi:10.1103/PhysRev.166.879.